Acta Biomaterialia 13 (2015) 150–158

Contents lists available at ScienceDirect

Acta Biomaterialia

journal homepage: www.elsevier.com/locate/actabiomat

Inhibition of osteolysis and increase of bone formation after local administration of siRNA-targeting *RANK* in a polyethylene particle-induced osteolysis model

L.A. Córdova [a,b,f,*], V. Trichet [a,b], V. Escriou [e], P. Rosset [a,b,c], J. Amiaud [a,b], S. Battaglia [a,b], C. Charrier [a,b], M. Berreur [a,b], R. Brion [a,b,d], F. Gouin [a,b,d], P. Layrolle [a,b], N. Passuti [a,b,d], D. Heymann [a,b,d]

[a] *INSERM, UMR 957, 1 rue Gaston Veil, 44035 Nantes Cedex 1, France*
[b] *University of Nantes, Nantes Atlantique Universities, Laboratory of Pathophysiology of Bone Resorption and Therapy of Primary Bone Tumours, 1 rue Gaston Veil, 44035 Nantes Cedex 1, France*
[c] *Tours University Hospital, François Rabelais, 37044 Tours Cedex 9, France*
[d] *Nantes University Hospital, 1 place Alexis-Ricordeau, 44093 Nantes Cedex 1, France*
[e] *UTCBS CNRS UMR 8258 INSERM UMR-S 1022, 4 avenue de l'Observatoire, 75006 Paris, France*
[f] *Department of Oral and Maxillofacial Surgery, San Borja Arriaran University Hospital, Faculty of Dentistry, University of Chile—CONICYT, Sergio Livingstone Polhammer 943, Independencia, Santiago, Chile*

ARTICLE INFO

Article history:
Received 5 June 2014
Received in revised form 25 October 2014
Accepted 28 October 2014
Available online 20 November 2014

Keywords:
siRNA
Polyethylene particle-induced osteolysis
Wear debris
Osteoclast

ABSTRACT

Receptor activator of nuclear factor kappa-B (RANK) and RANK-ligand are relevant targets for the treatment of polyethylene particle-induced osteolysis. This study assessed the local administration of siRNA, targeting both human *RANK* and mouse *Rank* transcripts in a mouse model. Four groups of mice were implanted with polyethylene (PE) particles in the calvaria and treated locally with 2.5, 5 and 10 μg of *RANK* siRNA or a control siRNA delivered by the cationic liposome DMAPAP/DOPE. The tissues were harvested at day 9 after surgery and evaluated by micro-computed tomography, tartrate-resistant acid phosphatase (TRAP) immunohistochemistry for macrophages and osteoblasts, and gene relative expression of inflammatory and osteolytic markers. 10 μg of *RANK* siRNA exerted a protective effect against PE particle-induced osteolysis, decreasing the bone loss and the osteoclastogenesis, demonstrated by the significant increase in the bone volume ($P < 0.001$) and by the reduction in both the number of $TRAP^+$ cells and osteoclast activity ($P < 0.01$). A bone anabolic effect demonstrated by the formation of new trabecular bone was confirmed by the increased immunopositive staining for osteoblast-specific proteins. In addition, 5 and 10 μg of *RANK* siRNA downregulated the expression of pro-inflammatory cytokines ($P < 0.01$) without depletion of macrophages. Our findings show that *RANK* siRNA delivered locally by a synthetic vector may be an effective approach for reducing osteolysis and may even stimulate bone formation in aseptic loosening of prosthetic implants.

1. Introduction

During the periprosthetic osteolysis process, wear particles released from bearing surfaces result in a local inflammatory response challenged by proinflammatory macrophages (M1) that produce interleukin-1 (IL-1) and tumour necrosis factor-alpha (TNF-α) [1]. The largest particles (>10 μm) coated with proteins may act as damage-associated molecular pattern molecules (DAMPs) and are sensed by macrophagic toll-like-receptors (TLRs) [2–4], leading to the activation of an innate inflammatory immune response such as a "foreign body reaction" [5,6]. Otherwise, the smallest particles (<10 μm) and ions are up taken, activating the NACHT, LRR and PYD domains-containing protein 3 (NALP3) inflammasome, leading to an adaptive immune response [3,5–7]. Both immune pathways activate the transcription factors NF-kB and NF-IL), increasing synthesis of the receptor activator of nuclear factor kappa-B ligand (RANKL) and pro-inflammatory cytokines (IL-1β, IL-6 and TNF-α) [8,9]. These cytokines were recognized as the main molecules responsible for maintaining the periprosthetic inflammatory environment and for increased osteoclastogenesis [8].

* Corresponding author at: INSERM UMR957, Pathophysiology of Bone Resorption and Therapy of Primary Bone Tumours, Faculty of Medicine, 1 rue Gaston Veil, 44035 Nantes cedex 1, France. Tel.: +33 272 641 132; fax: +33 240 412 860.
E-mail address: dominique.heymann@univ-nantes.fr (L.A. Córdova).

http://dx.doi.org/10.1016/j.actbio.2014.10.042
1742-7061/

Inhibition of the RANKL–RANK axis is an efficient therapeutic approach for decreasing osteoclast differentiation/activation. Anti-resorptive drug-based therapies, such as bisphosphonates and the anti-RANKL monoclonal antibody (Denosumab™), have evolved from experimental models of osteolytic bone diseases [10–13] to clinical uses [14–16]. In addition, new inhibitors, such as small peptides designed to target a specific region of the RANK membrane, are currently in preclinical development [17]. The prevention of bone loss by blocking the RANK–RANKL axis was reported in an experimental model of particle-induced osteolysis using a recombinant protein of RANK (RANK-Fc) [18] and by inducing the osteoclast apoptosis using zoledronic acid (ZOL) [19]. Despite these encouraging preclinical results, they have still not been transferred to clinical use [20].

Small interference ribonucleic acid (siRNA) regulates the synthesis of proteins by means of a specific gene silencing mechanism [21–23]. The use of siRNA-based therapy is a specific and biocompatible approach that has led to significant advances in cancer, age-related macular degeneration and viral diseases [24]. Two key aspects need to be considered in this strategy: the identification of clinically relevant targets and the use of efficient delivery vectors. Targeting of the key RANKL–RANK axis was first reported in vitro in murine cells by Wang et al. [25] and Ma et al. [26] with effective inhibition of *Rank* expression, osteoclast differentiation and osteolysis using *Rank*-siRNAs and *Rank*-shRNAs, respectively, which target the mouse *Rank* transcript [25–27]. The systemic delivery of therapeutic siRNAs using biological and synthetic vectors was reported in bone disease experimental models, including bone-metastatic cancer (targeting Luciferase (LucF) and delivered by atelocollagen) [28] and rheumatoid arthritis (targeting *TNF-α*, *IL-1ß*, *IL-6* and *IL-18* and delivered by the cationic liposome DMAPAP/DOPE) [29,30]. Similarly, a siRNA targeting of the type I bone morphogenetic protein receptor transcript (*BMPR-IB*) systemically delivered by a recombinant adenoviral vector was reported [31]. However, the nature of aseptic loosening by wear debris seems to be a confined condition that requires a local intervention. The local delivery of siRNAs is then a logical strategy for bypassing the anatomical barriers and optimizing its biotransformation during its transport. In this context, the local delivery of *Rankl*-siRNA by the cationic liposome DMAPAP/DOPE in a murine model of osteosarcoma [32] and a local lentiviral delivery of *β110*-siRNA, targeting a subunit of the PI3K/AKT pathway in a particle-induced osteolysis model, were reported [33]. However, there are no scientific reports using siRNA-based technology targeting the key RANKL–RANK axis by local delivery using a synthetic vector in an in vivo model. We hypothesized that siRNA targeting *RANK*, locally delivered in situ by a cationic liposome might be an effective approach for inhibiting osteoclastogenesis in vivo. The aim of our study was to unveil the therapeutic effect of three doses of siRNA targeting both human *RANK* and mouse *Rank* transcripts (*RANK*-811 siRNA) in a mouse model of polyethylene (PE) particle-induced osteolysis.

2. Material and methods

2.1. SiRNAs

All siRNAs were ordered from Eurogentec (Angers, France) with 3′ overhanging dTdT and with annealed sense and reverse strands. The primer sequence sense strand 5′-GUGGAAAUAAGGAGUCCUC-3′ was designed to target *Homo sapiens RANK* mRNA (NM_003839; Tumour Necrosis Factor Receptor Superfamily 11A, TNFRSF11A) at start positions 811 and was named *RANK*-811. The antisense strand of *RANK*-811 siRNAs presents perfect complementarity with *Mus musculus Rank* mRNA (NM_009399.2) at start positions 804. *RANK*-811 siRNA was selected based on its efficacy for decreasing *RANK* expression in *RANK*-overexpressing human embryonic kidney 293 (HEK 293) cells [17] and *Rank* in murine RAW 264.7 monocytic cells (American Type Culture Collection, Promochem, Molsheim, France) (Supplementary Information Fig. S1).

The siRNA duplex (sense strand 5′-UUCUCCGAACGUGUCACGU-3′) which did not show significant homology with any mouse mRNA sequence according to BLAST database searches, was used as a negative control and designated Ct-siRNA. A previously validated siRNA (*LucF*-siRNA sense strand 5′-CUUACGCUGAGUACUUCGA-3′) was used in vivo as an innocuous siRNA [32].

2.2. Particles of polyethylene

Pure PE particles (Ceridust 3610™) were purchased from Clariant (Gersthofen, Germany). The morphology of particles was assessed by scanning electron microscopy (JEOL, model 6400F). The particle size and distribution were determined by five consecutive measurements obtained with a Coulter Counter™ (Beckman Coulter Inc., USA). The mean size particle was 7.23 μm and with a distribution of d10 = 1.15, d25 = 3.94, d50 = 7.14, d75 = 10.28 and d90 = 13.05. To eliminate endotoxins, the particles were washed in ethanol, dried and then aliquoted until use [34]. Endotoxin levels were measured using a quantitative Limulus Amebocyte Lysate (LAL) assay (Lonza, Belgium). The threshold of positivity was 0.25 EU ml^{-1}.

2.3. Implantation of polyethylene particles in mouse calvaria

The mice (Elevages Janvier, Le Genest Saint Isle, France) were housed in pathogen-free conditions at the Experimental Therapy Unit (Faculty of Medicine, Nantes) in accordance with the institutional guidelines of the French Ethical Committee (CEEA PdL 06 ethical committee, authorization no. 1280.01) and under the supervision of the authorized investigators. All surgical procedures were also performed according to international ethical guidelines for animal care (authorization no. 2012-198). Twenty-one C57BL/6 male mice (Janvier, Le Genest-Saint Isle, France) aged 10 weeks were randomly divided in two groups (Table 1). Eighteen of the mice were surgically implanted using the adapted mouse calvaria model [35] with 20 mg of dried PE particles (PE-implanted group). Briefly, under general anaesthesia (2–3% isofluorane in 100% oxygen at flow rate of 1 l min^{-1}), a 0.5 × 0.5 cm^2 area of periosteum was exposed by a midsagittal incision in previously shaved and aseptic head skin (Betadine, France). The dried PE powder was uniformly spread over the periosteum with a sterile surgical spoon. The surgical approach was carefully closed with 5-0 non-absorbable sutures. A subcutaneous injection of buprenorphine (Buprecar 0.1 mg kg^{-1}) was performed after the surgical procedure (Palier 1 protocol). One group of three mice underwent the same surgical procedure but without the PE particle implantation (Sham group).

2.4. Local injections of formulated siRNAs

For in vivo injections, siRNAs were premixed with an equal quantity of a deoxyribonucleic acid (DNA) adjuvant in 150 mM sodium chloride as described in Ref. [36] and mixed with an equivalent volume of cationic liposome DMAPAP/DOPE at a ratio of 6 nmol of cationic lipid per microgram of nucleic acid as previously described [37]. The lipoplexes were formed at room temperature for at least 30 min. Injections of 50 μl of lipoplexes containing 2.5, 5 or 10 μg of siRNAs were used in vivo.

The PE-implanted mice were randomly divided in four groups which received siRNA injections, while the Sham group (non-implanted; $n = 3$) received 50 μl of saline solution (NaCl 0.9%) (Table 1). Three groups of PE-implanted mice received a total of

Table 1
Experimental design. Number of mouse or sample included per group or per assay.

Treatment	Non-implanted	PE-implanted			Total no. of animals
	Sham NaCl	*LucF* siRNA	*RANK*-811 siRNA		
Dose (μg)		2.5	2.5	5	10	
Micro-CT	3	3	5	5	5	
Histology	3	3	5	5	5	
RT-qPCR	3	3	3	3	3	
Animals per group	3	3	5	5	5	21

three injections (at days 1, 4 and 7 after surgery) in the calvaria site, of either 2.5 or 5 or 10 μg of *RANK*-811 siRNA and respectively named PE-2.5 μg *RANK*-811 siRNA ($n = 5$), PE-5 μg *RANK*-811 siRNA ($n = 5$) and PE-10 μg *RANK*-811 siRNA group ($n = 5$). One PE-implanted group received three injections of 2.5 μg *LucF*-siRNA and was named the PE-2.5 μg *LucF*-siRNA group ($n = 3$). The injection site was determined intermediate to the full cephalocaudal length of the sutured surgical approach and 2 mm laterally to the right of it. The inclination of the 26-gauge needle was oblique, pointing medially until a soft contact with the bone surface was made. A continuous and slow pressure injection, to avoid the reflow of injected solution, was performed. All animals were killed by cervical dislocation following isofluorane anaesthesia at day 9 after the surgical procedure.

2.5. Micro-computed tomography assessment

The analysis of bone microarchitecture was performed in fixed calvariae at the time corresponding to the necropsy (day 9) using a high-resolution X-ray micro-computed tomography (micro-CT) system for small-animal imaging (SkyScan-1076, SkyScan, Kontich, Belgium) (Table 1). All calvariae were scanned using the same parameters (pixel size 9 μm, 50 kV, 0.5 mm Al filter and 0.8° of rotation step). Three-dimensional reconstruction and quantification of bone parameters were performed in a cylindrical volume of interest (VOI) (ratio 0.5 mm, height 1.143 mm, VOI = 0.89 mm^3; Fig. 2A) using ANT and CTvol software (Skyscan). The assessment of the bone volume density was measured by the fraction of the VOI (i.e. the total volume, TV) that is occupied by mineralized bone (bone volume, BV) (BV/TV) expressed as a percentage (%).

2.6. Histological analysis

Harvested calvariae were fixed in 4% buffered formaldehyde for 24 h and decalcified with 4.13% ethylenediaminetetraacetic acid (EDTA) and 0.2% paraformaldehyde in phosphate-buffered saline (PBS) for 96 h using a KOS microwave histostation (Milestone, Kalamazoo, MI, USA) before embedding in paraffin (Table 1). Six coronal 4 μm thick sections were obtained from three levels of middle calvaria (each one separated by 300 μm). All slides were stained for tartrate-resistant acid phosphatase (TRAP) to identify osteoclasts by 1 h incubation in a 1 mg ml^{-1} naphthol AS-TR phosphate, 60 mmol l^{-1} *N*,*N*-dimethylformamide, 100 mmol l^{-1} sodium tartrate and 1 mg ml^{-1} Fast Red TR salt solution (Sigma Aldrich, Saint Quentin Fallavier, France) and counterstained with haematoxylin.

For immunohistochemistry, histological sections were treated with citrate buffer at pH 6 for antigen unmasking and with goat serum 5%, BSA 1% diluted in 1× TBS pH 7.6 for blocking of non-antibody-specific sites. The immunostaining for F4-80 was performed using rabbit monoclonal anti-F4-80 antibody (1/150 overnight at 4 °C; Abcam, Cambridge, MA, USA) and goat anti-rabbit biotinylated (Dako, Glostrup, Denmark) as a secondary antibody. Immunostaining for alkaline phosphatase (ALP) was carried out using rabbit monoclonal anti-ALP antibody and goat anti-rabbit biotinylated (Dako) as a secondary antibody. Following incubation with a streptavidin/peroxidase kit (1/200, Dako), antibody detection was made with a liquid DAB-substrate chromogen system (Dako).

Histological images were acquired with a digital slide scanner (NanoZoomer 2.0-RS, Hamamatsu, Japan). The region of interest (ROI) corresponded to a rectangular area (1.7 mm^2, 1.74 mm wide and 980 mm high, 1913 × 582 pixels) centred in the middle sagittal suture and comprising the full thickness of the parietal bones. Two independent pathologists performed a qualitative assessment based on morphological criteria. Quantification of $TRAP^+$ cells was assessed with ImageJ software (NIH, Bethesda, MD, USA) and expressed as the percentage of osteoclasts (estimated from $TRAP^+$ area) in the defined ROI area. This method was recently published in Refs. [38–40].

2.7. RNA extraction from calvaria tissue and quantitative real-time polymerase chain reaction (qRT-PCR)

Total RNA was extracted from three implanted calvaria samples of each group using homogenizer Ika Ultra-Thurax T 25 (Janke and Kunkel) and TRIzol reagent (Invitrogen) (Table 1). Synthesis of the first strand of complementary DNA and the polymerase chain reaction were carried out in triplicate using the same protocol as described above. The listed oligonucleotides were used to amplify *Mus musculus* receptor activator of nuclear factor kappa-B (*Rank*, 5′-TGCAGCTCTTCCATGACACTG-3′ and 5′-CAGCCACTACTACCACAGAGATG-3′), Cathepsin K (*CathK*, 5′-GGAGGCGGCTATATGACCA-3′ and 5′-GATCTATGTCCTCACCGAACG-3′), tumour necrosis factor alpha (*Tnf-α*, 5′-GGGTGATCGGTCCCCAAAGGGA-3′ and 5′-TGGTTTGCTACGACGTGGGCTAC-3′), interleukin-6 (*Il-6*, 5′-TAGTCCTTCCTACCCCAATTTCC-3′ and 5′-TTGGTCCTTAGCCACTCCTTC-3′), interleukin-1 (*Il-1β*, 5′-TTGACGGACCCCAAAAGAT-3′ and 5′-GATGTGCTGCTGCGAGATT-3′), cytochrome c-1 (*Cyc 1*, 5′-TGTGCTACACGGAGGAAGAA-3′ and 5′-CATCATCATTAGGGCCATCC-3′) and 60S ribosomal protein L19 (*Rpl19*, 5′-TCGTTGCCGGAAAAACAC-3′ and 5′-AGGTCACCTTCTCAGGCATC-3′). *Cyc* and *Rpl19* were used as housekeeping genes. Target gene expression was normalized to a housekeeping gene in respective samples as an internal standard, and the comparative cycle threshold method was used to calculated relative quantification of target messenger RNAs. Analyses were then performed using the Vandesompele method [41].

2.8. Statistical analysis

All analyses were performed using GraphPad InStat version 3.02 software (GraphPad Software, La Jolla, CA, USA). In vitro experimentation and micro-CT results were analyzed with the unpaired non-parametric Mann–Whitney *U*-test using two-tailed *P* values. Each *RANK* siRNA group was compared independently with the *LucF* siRNA group. The histological results were analyzed with

ANOVA and an unpaired parametric two-tailed *t*-test. Results are given considering a *P* value <0.05 as representing significance.

3. Results

3.1. RANK-811 siRNA prevents the bone loss induced by implanted PE particles by inhibiting osteoclastogenesis and osteoclast activation

A first assessment of the anti-resorptive effect of *RANK-811* siRNA in vivo at day 9 after implantation of PE particles using micro-CT showed that the inner cortical of the calvaria was protected from osteolysis in the groups treated with 5 or 10 μg of *RANK*-811 siRNAs. However, an increase in the bone volume was only observed at a dose of 10 μg of *RANK*-811 siRNA (BV/TV = 19.11% ± 2.3) compared to the control siRNA (BV/TV = 10.57% ± 0.6; $P = 0.006$). However, severe bone loss of the inner cortical area was observed for the group treated with 2.5 μg of *RANK*-811 siRNAs (Fig. 1A, B).

TRAP staining revealed that osteoclasts detected in the groups injected with 5 or 10 μg of *RANK*-811 siRNAs were smaller than those in the groups injected with 2.5 μg *LucF*- or *RANK*-811 siRNAs (Fig. 2A). In addition, *RANK*-811 siRNAs inhibited osteoclast differentiation in a dose-dependent manner. Indeed, the percentage of TRAP-positive cells was reduced by 70% with 2.5 μg *RANK*-811 siRNA ($P = 0.003$) and by 90% with 5 ($P = 0.0009$) and 10 μg ($P = 0.0007$) *RANK-811* siRNA administration (Fig. 2B).

The inhibitory effect of *RANK*-811 siRNAs on osteoclast activity was also confirmed by the downregulation of *Rank* expression after 5 ($P = 0.0001$) and 10 μg ($P = 0.006$) *RANK-811* siRNA administration (Fig. 2B). In addition to the inhibition of osteoclastogenesis, *RANK*-811 siRNAs was also decreased *Cathepsin K* expression (Fig. 2B), demonstrating the inhibition of the osteoclast activity with 5 ($P = 0.001$) and 10 μg ($P = 0.001$) *RANK-811* siRNA. In contrast, 2.5 μg *RANK-811* siRNA did not modify *Rank* expression (not significant (NS)) and induced an increase of *Cathepsin* K expression ($P = 0.01$) (Fig. 2B).

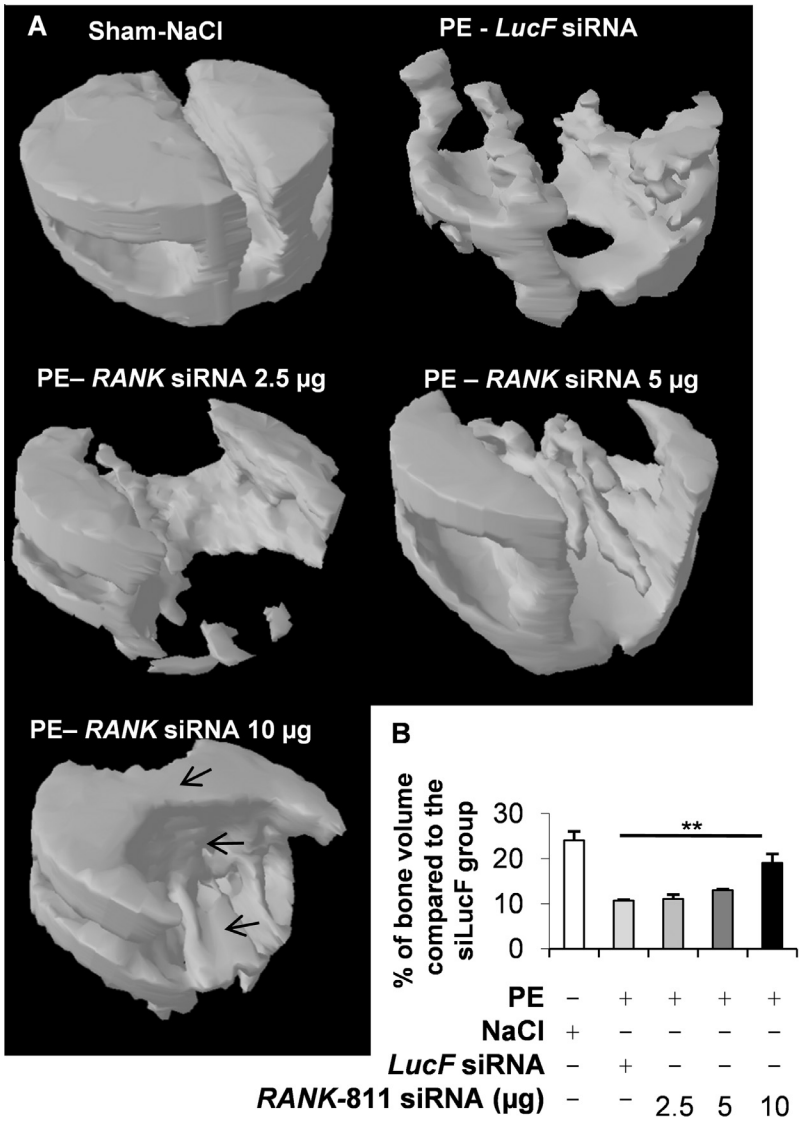

Fig. 1. ***RANK***-811 siRNA exhibits a significant protective effect against PE particle-induced osteolysis in vivo. PE particles were implanted or not (Sham-NaCl) over the periosteum of calvaria for 9 days. Increasing doses (2.5, 5 and 10 μg) of *RANK*-811 siRNA were injected locally and bone quantity was followed, compared to the control *LucF* siRNA. PE particle-induced osteolysis and the efficacy of *RANK*-811 siRNA was followed qualitatively by micro-CT scan (A) and quantitatively determined by the measure of the BV/TV (B). Bone preserved areas were recognized in spongy bone as well as in external and inner corticals (black arrows). $^{**}P < 0.01$.

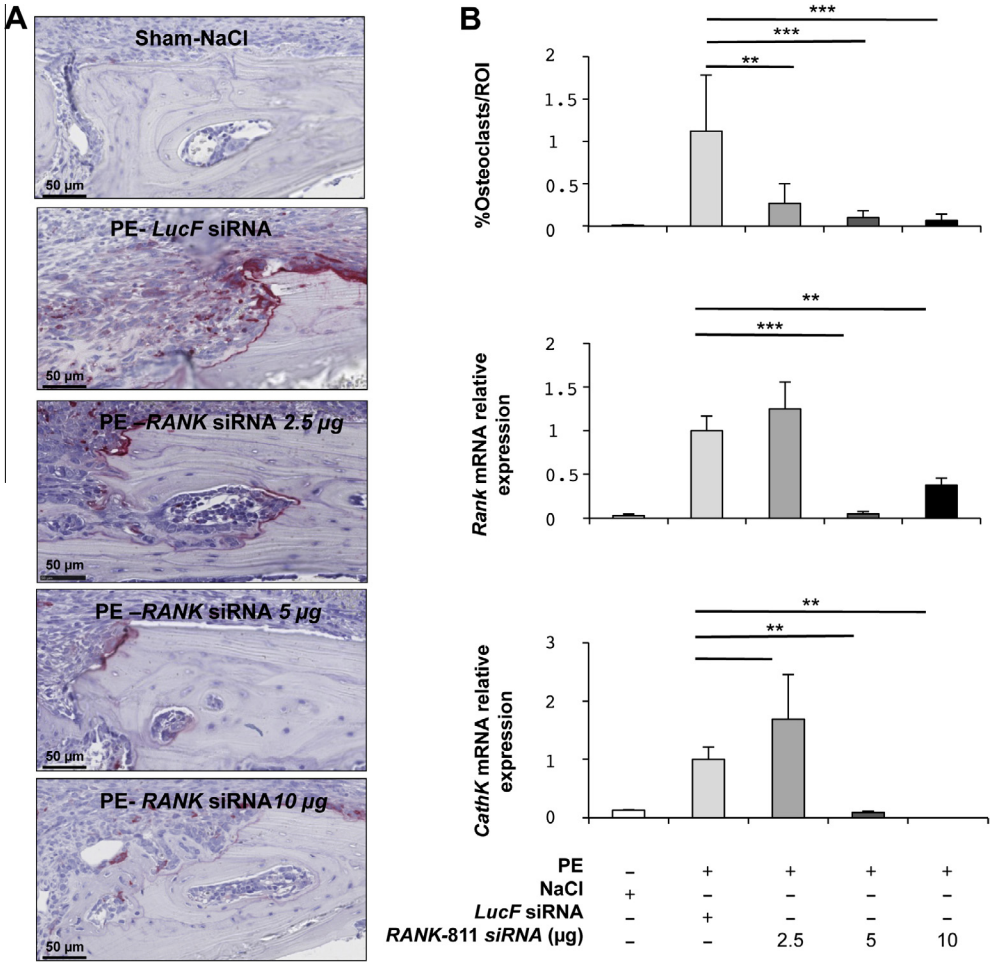

Fig. 2. ***RANK***-811 siRNA inhibits in vivo the number of osteoclasts in a dose dependent manner. PE particles were implanted or not (Sham-NaCl) over the periosteum site of calvaria for 9 days. Increasing doses (2.5, 5 and 10 µg) of *RANK*-811 siRNA were injected locally and bone loss intensity was followed compared to the control *LucF* siRNA. Osteoclasts were detected by TRAP staining (A) and their number was quantified by the percentage of osteoclasts/ROI (B upper). *Rank* (B middle) and *cathepsin K* (B lower) expression was determined by qRT-PCR from calvaria tissue explants compared to the *LucF* siRNA. $^{*}P < 0.05$; $^{**}P < 0.01$; $^{***}P < 0.001$.

3.2. Local treatment with the formulated siRNA induces an anabolic bone response characterized by the total renewal of osteoblastic cell lineage

PE-implanted mice exhibit osteonecrotic and osteolytic lesions. Thus, we confirmed the presence of empty lacunae, without osteocytes, in the external cortex of the calvaria of PE-implanted mice compared with non-implanted mice (Fig. 3A). However, characteristic osteocytes located in their cavities were observed in the inner cortex of the calvariae in all groups assessed (Fig. 3A). Interestingly, new bone formation was observed in the PE-implanted and siRNA-treated mice compared to the Sham group, as demonstrated by ALP (Fig. 3A) and osterix (Fig. 3B) positive immunostaining in the area of interest.

3.3. RANK-811. siRNA reduced the inflammatory environment without depletion of macrophages

Because it is known that wear debris induces an inflammatory reaction [7,42], we assessed the consequence of a *Rank* blockade on the inflammatory process. Histological analysis showed that the implantation of PE particles resulted in a reaction characterized by the thickening of an inflammatory membrane more infiltrated by cells compared with the non-implanted group (Fig. 4A). F4/80^{+} macrophages were detected either in the Sham group (loosely distributed in the subcutaneous connective tissue) as well as in the implanted groups (highly localized within the inflammatory membrane and surrounding the implanted particles) (Fig. 4A). Similarly, we observed the proinflammatory effect of PE particles by the increased expression of proinflammatory cytokines genes (*Tnf-α*, *Il-6* and *Il-1β*) from the PE-*LucF*-siRNA group compared with the Sham–NaCl group (Fig. 4B). We observed that the injections of 2.5 µg *RANK*-811 siRNAs decreased *Tnf-α* expression ($P = 0.007$) and slightly increased the expression of *Il-1β* ($P = 0.04$) compared to the *LucF* siRNA injections. *Il-6* expression was not modulated using the same dose of siRNA (NS). In contrast, the injections of 5 and 10 µg of *RANK*-811 siRNAs decreased the expression of *Tnf-α* ($P = 0.0001$ and $P = 0.0002$, respectively), *Il-6* ($P = 0.0001$ and $P = 0.0009$, respectively) and *Il-1β* ($P = 0.0001$ and $P = 0.008$, respectively) (Fig. 4B). Interestingly and despite the down-regulation of proinflammatory genes associated with the injection of 5 and 10 µg of *RANK*-811 siRNA and the variable response of the same parameters for the same genes using 2.5 µg *RANK*-811 siRNA, the macrophage infiltration was not repressed (Fig. 4A).

4. Discussion

Targeting the components of the triad OPG/RANKL/RANK by interference of RNA seems to be a promising approach. Experimental studies blocking RANKL–RANK signalling by siRNAs targeting

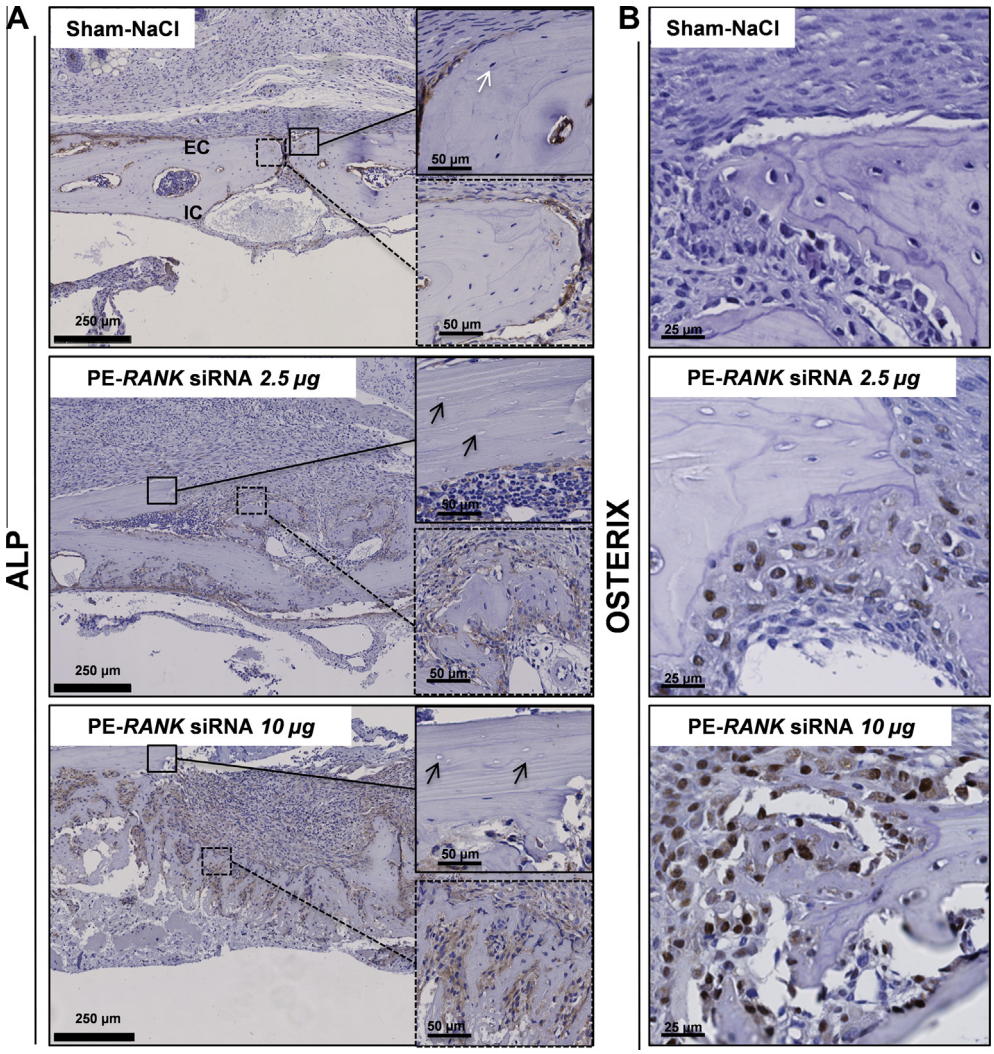

Fig. 3. ***RANK***-811 siRNA induces the renewal of osteoblastic cell lineage after osteolytic/osteonecrotic stimulus induced by PE. PE particles were implanted or not (Sham-NaCl) over the periosteum of calvaria for 9 days. Increasing doses (2.5, 5 and 10 μg) of *RANK*-811 siRNA were injected locally and bone formation was followed compared to the Sham group. ALP (A) and Osterix (B) immunostaining was used to detect mature osteoblasts and pre-osteoblasts, respectively. Empty lacunae were recognized in external cortex of calvaria (black arrows in A, continuous zoomed window). ALP^+ (A, discontinuous zoomed windows, middle and bottom) and OSX^+ (B, middle and bottom) cells associated with new trabecular bone were detected in central area from the edges of external cortex and internal cortex.

M. musculus Rank have previously been reported in in vitro systems with an effective inhibition of *Rank* expression, osteoclast differentiation and osteolysis [25–27]. Furthermore, the efficacy of siRNAs targeting *Rankl* was reported in in vitro culture of *RANKL*-expressing HEK 293 cells and in a murine model of osteosarcoma [32,37]. Our study provides strong evidence of the efficacy of three formulated cross-species sequences of *RANK* siRNAs in both human *RANK*-expressing HEK 293 cells and in murine RAW 264.7 cells in vitro (Fig. S1). Then, once the down-regulation of *RANK* and *Rank* was confirmed, we selected the most efficient sequence among the three evaluated (*RANK*-811 siRNA with 48.7% of inhibition) to assess its effect on osteolysis in vivo (Fig. S1).

Our study shows for the first time an effective inhibition of particle-induced osteolysis in an in vivo model using a *RANK*-directed siRNA sequence. We observed a large reduction in the number of $TRAP^+$ activated cells in the parasagittal area on implanted calvariae using three different doses of *RANK*-811 siRNAs. This observation revealed a high ability of the osteoclast precursors to uptake the injected lipoplex (*RANK*-811 siRNA with synthetic vector, cationic liposome DMAPAP/DOPE and plasmid). This synthetic vector has also shown efficacy in the local delivery of formulated *Rankl*-directed siRNA by intra-tumour injection in previous reports [32,37]. Moreover, Khoury et al. [29,30], reported a successful systemic delivery of siRNAs targeting proinflammatory cytokines (*Tnf-α*, *Il-1β*, *Il-6* and *Il-18*) in a mouse model of rheumatoid arthritis using the same siRNA formulation [29,30].

While the doses of 5 and 10 μg of *RANK*-811 siRNAs decreased the number of $TRAP^+$ cells and the expression of osteolytic genes (*Rank* and *Cathepsin K*), confirming the inhibition of osteoclastogenesis and osteolysis, we observed a contradictory response with the dose of 2.5 μg. These findings may be explained by an imbalance between the amount of *Rank* transcript and the weak dose of siRNA (2.5 μg). Supporting this observation, the volumetric assessment by micro-CT showed that only the maximal dose assessed, 10 μg of *RANK*-811 siRNA, prevented bone loss compared to the control group (PE-*LucF*-siRNA). Furthermore, a major effectiveness of lipoplex in the external cortical area rather than in the inner cortical area of the calvaria was also observed. These differences may be explained by a reduced diffusion of the injected volume to the inner cortical area due to the modified local anatomy (eroded surface of bone and trabecular spaces in the diploe), by the local inflammatory reaction and/or the viscosity of the

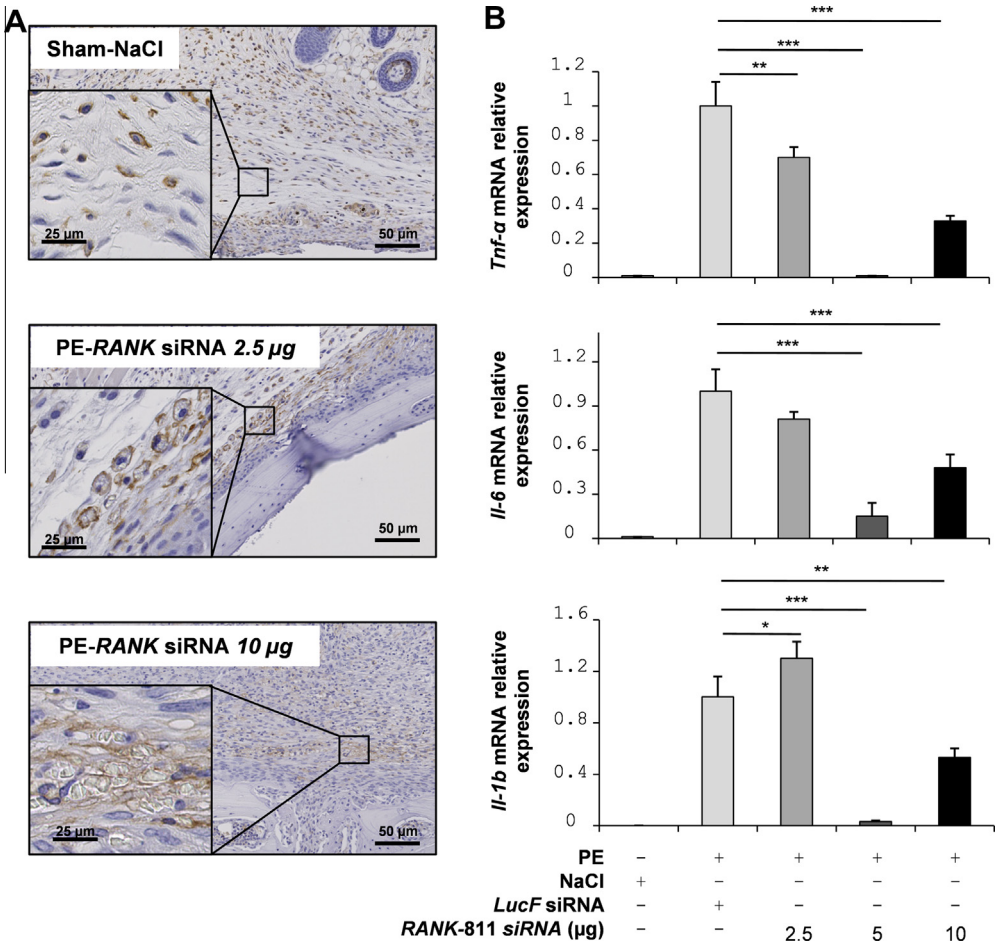

Fig. 4. ***RANK***-811 siRNA does not modulate the invading macrophages. PE particles were implanted or not (Sham-NaCl) over the periosteum of calvaria for 9 days. Increasing doses (2.5, 5 and 10 μg) of *RANK* siRNA-811 were injected locally and inflammatory status was followed compared to the control *LucF* siRNA. Macrophages were identified by anti-F4-80 antibody in all groups (implanted and sham) mice (A). The relative expression of *Tnf-α*, *Il-6* and *Il-1β* was determined in explanted tissues by qRT-qPCR. While 5 and 10 μg *RANK*-811 siRNA decreases the expression of pro-inflammatory *Tnf-α*, *Il-6* and *Il-1β* cytokines, the dose of 2.5 μg induces a variable response decreasing *Tnf-α*, maintaining *Il-6* and increasing *Il-1β* expression. (B). $^{*}P < 0.05$; $^{**}P < 0.01$; $^{***}P < 0.001$.

lipoplex. The present results were consistent with a direct antiresorptive effect of *RANK*-811 siRNA, presumably on RANK^{+} pre-osteoclasts and/or mature osteoclasts, demonstrated by the inhibition of osteoclastogenesis and the decrease of osteoclast activity (Figs. 1 and 2) similarly to the zoledronic acid treatment (Fig. S2).

Interestingly, the unexpected bone formation observed in siRNA-treated mice suggests that the injection of this lipoplex might create a favourable local anabolic microenvironment. Thus, a complete renewal of osteoblastic lineage characterized by a sequence of localized osteolysis/osteonecrosis induced by PE particles, followed by a pulse of bone formation induced by the *RANK*-811 siRNA may be proposed. The osteogenic signs observed in the central area of calvariae may be secondary to the inflammatory microenvironment generated by particle implantation and/or possibly, the immunogenic effect of lipoplex. The link between inflammation and osteogenesis was recently proposed and might be regulated by oncostatin M signalling produced by monocytes/macrophages [43]. In addition, a STAT3 activation in mesenchymal stem cells was reported [44]. Further studies need to be performed to elucidate the osteogenic effect showed in our report.

On the other hand, the dramatic inhibition of the expression of proinflammatory cytokines in harvested tissues of *RANK*-811 siRNA-treated mice (including RANK^{+} pre-osteoclasts and osteoclasts) could also actively participate in the modulation of the inflammatory response. We also observed the persistence of macrophages both in non-implanted (Sham) and in *RANK*-811 siRNA-treated groups. While those observed in the Sham group exhibited a heterogeneous distribution in connective tissue and could be associated with the inflammatory process after a surgical approach, those observed in the *RANK*-811 siRNA-treated groups were always closely related to the PE particles (presumably phagocytosed by them). This fact could be related with the paradoxical rise of the cytokine expression observed with the highest dose (10 μg) of siRNA. A potential immunoactivation role of the lipoplex [45,46] (or some of its components, i.e. cationic liposome or nucleic acids) could explain these findings. However, in a previous study, we showed that the same construct used in an intra-osseous site did not activate the systemic immune response [32]. These contradictory data reinforce our hypothesis for the existence of non-identified cellular sources for pro-inflammatory mediators (i.e. osteoclast precursors, dendritic cells, lymphoid cells and/or stromal cells).

The difficulty in determining the cell(s) type(s) that effectively internalize(s) the *RANK*-811 siRNA administered is the first limitation of the present study. The use of carboxyfluorescein-labelled-siRNAs (FAM-siRNAs) would allow the identification of the cells incorporating this siRNA. The interest of FAM-siRNAs delivered by cationic liposomes to detect its trafficking in bone tissue was previously shown by Zhang et al. [47]. In addition, the cationic

liposome used in Zhang et al.'s study has been combined with a peptide for delivering siRNAs specifically to bone-forming surfaces. In our study, the liposome DMAPAP/DOPE was not functionalized for such bone targeting. However, we observed a delivery of *RANK*-siRNAs by the cationic liposome in osteoclasts of implanted calvaria as demonstrated by the marked decrease in the $TRAP^+$ cell number. Moreover the internalization of siRNAs using the cationic liposome DMAPAP/DOPE was confirmed in monocyte/macrophages in a murine model of rheumatoid arthritis [30]. Further studies will be necessary to reveal the specific cell(s) that uptake *RANK*-811 siRNA and to determine the intracellular sites of interaction. Finally, while we present consistent evidence about the anti-resorptive effects of siRNA in experimental conditions, the promise of using anti-inflammatory and bone anabolic effects needs to be confirmed in a large number of samples.

5. Conclusions

Following local treatment with three doses of *RANK*-811 siRNA delivered by the cationic lipid DMAPAP/DOPE in a PE particle-induced osteolytic mouse model, the bone volume was preserved with the dose of 10 μg. We also observed that 5 and 10 μg *RANK*-811 siRNA dramatically decreased the osteoclastogenesis, osteolysis and inflammation, while the dose of 2.5 μg revealed contradictory effects. However, we showed consistent microarchitectural, histological and molecular findings to support the effectiveness of a siRNA-based approach locally delivered targeting *RANK* in the prevention of experimental osteolysis induced by PE particles. Further studies will be necessary to specify the optimal conditions for siRNA administration, the site of interaction and potential side effects. This study strengthens the concept for the usefulness of siRNA-based therapy targeting *RANK*, an innovative actor in the pathophysiology of particle-induced osteolysis.

Acknowledgements

Financial support for this research was provided by the Agence Nationale de la Recherche, Grant 2007 Pathophysiology of Human Diseases Project No. RO 7196N, INSERM, University of Nantes, France and by CONICYT—Becas Chile, Chile.

Appendix A. Supplementary data

Supplementary data associated with this article can be found, in the online version, at http://dx.doi.org/10.1016/j.actbio.2014.10.042.

References

[1] Ingham E, Fisher J. The role of macrophages in osteolysis of total joint replacement. Biomaterials 2005;26:1271–86. http://dx.doi.org/10.1016/j.biomaterials.2004.04.035.
[2] Fukata M, Vamadevan AS, Abreu MT. Toll-like receptors (TLRs) and Nod-like receptors (NLRs) in inflammatory disorders. Semin Immunol 2009;21:242–53. http://dx.doi.org/10.1016/j.smim.2009.06.005.
[3] Caicedo MS, Desai R, McAllister K, Reddy A, Jacobs JJ, Hallab NJ. Soluble and particulate Co-Cr-Mo alloy implant metals activate the inflammasome danger signaling pathway in human macrophages: a novel mechanism for implant debris reactivity. J Orthop Res Off Publ Orthop Res Soc 2009;27:847–54. http://dx.doi.org/10.1002/jor.20826.
[4] Pearl JI, Ma T, Irani AR, Huang Z, Robinson WH, Smith RL, et al. Role of the Toll-like receptor pathway in the recognition of orthopedic implant wear-debris particles. Biomaterials 2011;32:5535–42. http://dx.doi.org/10.1016/j.biomaterials.2011.04.046.
[5] Goodman SB. Wear particles, periprosthetic osteolysis and the immune system. Biomaterials 2007;28:5044–8. http://dx.doi.org/10.1016/j.biomaterials.2007.06.035.
[6] Pierre CA, Chan M, Iwakura Y, Ayers DC, Kurt-Jones EA, Finberg RW. Periprosthetic osteolysis: characterizing the innate immune response to titanium wear-particles. J Orthop Res 2010;28:1418–24. http://dx.doi.org/10.1002/jor.21149.
[7] Burton L, Paget D, Binder NB, Bohnert K, Nestor BJ, Sculco TP, et al. Orthopedic wear debris mediated inflammatory osteolysis is mediated in part by NALP3 inflammasome activation. J Orthop Res Off Publ Orthop Res Soc 2013;31:73–80. http://dx.doi.org/10.1002/jor.22190.
[8] Purdue PE, Koulouvaris P, Nestor BJ, Sculco TP. The central role of wear debris in periprosthetic osteolysis. HSS J Musculoskelet J Hosp Spec Surg 2006;2:102–13. http://dx.doi.org/10.1007/s11420-006-9003-6.
[9] Lin T, Tamaki Y, Pajarinen J, Waters HA, Woo DK, Yao Z, et al. Chronic inflammation in biomaterial-induced periprosthetic osteolysis: NF-κB as a therapeutic target. Acta Biomater 2014;10:1–10. http://dx.doi.org/10.1016/j.actbio.2013.09.034.
[10] Gasser JA, Ingold P, Venturiere A, Shen V, Green JR. Long-term protective effects of zoledronic acid on cancellous and cortical bone in the ovariectomized rat. J Bone Miner Res Off J Am Soc Bone Miner Res 2008;23:544–51. http://dx.doi.org/10.1359/jbmr.071207.
[11] Le Goff B, Soltner E, Charrier C, Maugars Y, Rédini F, Heymann D, et al. A combination of methotrexate and zoledronic acid prevents bone erosions and systemic bone mass loss in collagen induced arthritis. Arthritis Res Ther 2009;11:R185. http://dx.doi.org/10.1186/ar2877.
[12] Odri GA, Dumoucel S, Picarda G, Battaglia S, Lamoureux F, Corradini N, et al. Zoledronic acid as a new adjuvant therapeutic strategy for Ewing's sarcoma patients. Cancer Res 2010;70:7610–9. http://dx.doi.org/10.1158/0008-5472.CAN-09-4272.
[13] Moriceau G, Ory B, Gobin B, Verrecchia F, Gouin F, Blanchard F, et al. Therapeutic approach of primary bone tumours by bisphosphonates. Curr Pharm Des 2010;16:2981–7.
[14] Lacey DL, Boyle WJ, Simonet WS, Kostenuik PJ, Dougall WC, Sullivan JK, et al. Bench to bedside: elucidation of the OPG-RANK-RANKL pathway and the development of denosumab. Nat Rev Drug Discov 2012;11:401–19. http://dx.doi.org/10.1038/nrd3705.
[15] Orwoll ES, Miller PD, Adachi JD, Brown J, Adler RA, Kendler D, et al. Efficacy and safety of a once-yearly i.v. Infusion of zoledronic acid 5 mg versus a once-weekly 70-mg oral alendronate in the treatment of male osteoporosis: a randomized, multicenter, double-blind, active-controlled study. J Bone Miner Res Off J Am Soc Bone Miner Res 2010;25:2239–50. http://dx.doi.org/10.1002/jbmr.119.
[16] Leder BZ, Tsai JN, Uihlein AV, Burnett-Bowie S-AM, Zhu Y, Foley K, et al. Two years of denosumab and teriparatide administration in postmenopausal women with osteoporosis (the DATA Extension Study): a randomized controlled trial. J Clin Endocrinol Metab 2014:jc20134440. http://dx.doi.org/10.1210/jc.2013-4440.
[17] Téletchéa S, Stresing V, Hervouet S, Baud'huin M, Heymann M-F, Bertho G, et al. Novel RANK antagonists for the treatment of bone resorptive disease: theoretical predictions and experimental validation. J Bone Miner Res 2014:n/a–a. http://dx.doi.org/10.1002/jbmr.2170.
[18] Childs LM, Paschalis EP, Xing L, Dougall WC, Anderson D, Boskey AL, et al. In vivo RANK signaling blockade using the receptor activator of NF-kappaB:Fc effectively prevents and ameliorates wear debris-induced osteolysis via osteoclast depletion without inhibiting osteogenesis. J Bone Miner Res Off J Am Soc Bone Miner Res 2002;17:192–9. http://dx.doi.org/10.1359/jbmr.2002.17.2.192.
[19] Von Knoch M, Wedemeyer C, Pingsmann A, von Knoch F, Hilken G, Sprecher C, et al. The decrease of particle-induced osteolysis after a single dose of bisphosphonate. Biomaterials 2005;26:1803–8. http://dx.doi.org/10.1016/j.biomaterials.2004.06.010.
[20] Zeng Y, Lai O, Shen B, Yang J, Zhou Z, Kang P, et al. A systematic review assessing the effectiveness of alendronate in reducing periprosthetic bone loss after cementless primary THA. Orthopedics 2011:34. http://dx.doi.org/10.3928/01477447-20110228-09.
[21] Elbashir SM, Harborth J, Lendeckel W, Yalcin A, Weber K, Tuschl T. Duplexes of 21-nucleotide RNAs mediate RNA interference in cultured mammalian cells. Nature 2001;411:494–8. http://dx.doi.org/10.1038/35078107.
[22] Sijen T, Fleenor J, Simmer F, Thijssen KL, Parrish S, Timmons L, et al. On the role of RNA amplification in dsRNA-triggered gene silencing. Cell 2001;107:465–76. http://dx.doi.org/10.1016/S0092-8674(01)00576-1.
[23] Gherardini L, Bardi G, Gennaro M, Pizzorusso T. Novel siRNA delivery strategy: a new "strand" in CNS translational medicine? Cell Mol Life Sci CMLS 2013. http://dx.doi.org/10.1007/s00018-013-1310-8.
[24] Bora RS, Gupta D, Mukkur TKS, Saini KS. RNA interference therapeutics for cancer: challenges and opportunities (review). Mol Med Rep 2012;6:9–15. http://dx.doi.org/10.3892/mmr.2012.871.
[25] Wang Y, Grainger DW. SiRNA Knock-down of RANK signaling to control osteoclast-mediated bone resorption. Pharm Res 2010;27:1273–84. http://dx.doi.org/10.1007/s11095-010-0099-5.
[26] Ma R, Xu J, Dong B, Kauther MD, Jäger M, Wedemeyer C. Inhibition of osteoclastogenesis by RNA interference targeting RANK. BMC Musculoskelet Disord 2012;13:154. http://dx.doi.org/10.1186/1471-2474-13-154.
[27] Wang Y, Tran KK, Shen H, Grainger DW. Selective local delivery of RANK siRNA to bone phagocytes using bone augmentation biomaterials. Biomaterials 2012;33:8540–7. http://dx.doi.org/10.1016/j.biomaterials.2012.07.039.
[28] Takeshita F. Efficient delivery of small interfering RNA to bone-metastatic tumors by using atelocollagen in vivo. Proc Natl Acad Sci 2005;102:12177–82. http://dx.doi.org/10.1073/pnas.0501753102.

[29] Khoury M, Louis-Plence P, Escriou V, Noel D, Largeau C, Cantos C, et al. Efficient new cationic liposome formulation for systemic delivery of small interfering RNA silencing tumor necrosis factor α in experimental arthritis. Arthritis Rheum 2006;54:1867–77. http://dx.doi.org/10.1002/art.21876.

[30] Khoury M, Escriou V, Courties G, Galy A, Yao R, Largeau C, et al. Efficient suppression of murine arthritis by combined anticytokine small interfering RNA lipoplexes. Arthritis Rheum 2008;58:2356–67. http://dx.doi.org/10.1002/art.23660.

[31] Wang Y, Wu N-N, Hu M, Mou Y-Q, Li R-D, Chen L, et al. Inhibitory effect of adenovirus-mediated siRNA-targeting BMPR-IB on UHMWPE-induced bone destruction in the murine air pouch model. Connect Tissue Res 2012;53:528–34. http://dx.doi.org/10.3109/03008207.2012.702817.

[32] Rousseau J, Escriou V, Lamoureux F, Brion R, Chesneau J, Battaglia S, et al. Formulated siRNAs targeting Rankl prevent osteolysis and enhance chemotherapeutic response in osteosarcoma models. J Bone Miner Res Off J Am Soc Bone Miner Res 2011;26:2452–62. http://dx.doi.org/10.1002/jbmr.455.

[33] Huang J-B, Ding Y, Huang D-S, Zeng W-K, Guan Z-P, Zhang M-L. RNA Interference targeting p110β reduces tumor necrosis factor-alpha production in cellular response to wear particles in vitro and osteolysis in vivo. Inflammation 2013. http://dx.doi.org/10.1007/s10753-013-9636-9.

[34] Nich C, Langlois J, Marchadier A, Vidal C, Cohen-Solal M, Petite H, et al. Oestrogen deficiency modulates particle-induced osteolysis. Arthritis Res Ther 2011;13:R100. http://dx.doi.org/10.1186/ar3381.

[35] Nich C, Marchadier A, Sedel L, Petite H, Vidal C, Hamadouche M. Decrease in particle-induced osteolysis in ovariectomized mice. J Orthop Res 2010;28:178–83. http://dx.doi.org/10.1002/jor.20987.

[36] Rhinn H, Largeau C, Bigey P, Kuen RL, Richard M, Scherman D, et al. How to make siRNA lipoplexes efficient? Add a DNA cargo. Biochim Biophys Acta 2009;1790:219–30. http://dx.doi.org/10.1016/j.bbagen.2009.01.005.

[37] Rousseau J, Escriou V, Perrot P, Picarda G, Charrier C, Scherman D, et al. Advantages of bioluminescence imaging to follow siRNA or chemotherapeutic treatments in osteosarcoma preclinical models. Cancer Gene Ther 2010;17:387–97. http://dx.doi.org/10.1038/cgt.2009.89.

[38] Gobin B, Battaglia S, Lanel R, Chesneau J, Amiaud J, Rédini F, et al. NVP-BEZ235, a dual PI3K/mTOR inhibitor, inhibits osteosarcoma cell proliferation and tumor development in vivo with an improved survival rate. Cancer Lett 2014;344:291–8. http://dx.doi.org/10.1016/j.canlet.2013.11.017.

[39] Gobin B, Huin MB, Lamoureux F, Ory B, Charrier C, Lanel R, et al. BYL719, a new α-specific PI3K inhibitor: single administration and in combination with conventional chemotherapy for the treatment of osteosarcoma. Int J Cancer 2014:n/a–a. http://dx.doi.org/10.1002/ijc.29040.

[40] Lamoureux F, Baud'huin M, Rodriguez Calleja L, Jacques C, Berreur M, Rédini F, et al. Selective inhibition of BET bromodomain epigenetic signalling interferes with the bone-associated tumour vicious cycle. Nat Commun 2014;5. http://dx.doi.org/10.1038/ncomms4511.

[41] Vandesompele J, De Preter K, Pattyn F, Poppe B, Van Roy N, De Paepe A, et al. Accurate normalization of real-time quantitative RT-PCR data by geometric averaging of multiple internal control genes. Genome Biol 2002;3:RESEARCH0034.

[42] Rao AJ, Gibon E, Ma T, Yao Z, Smith RL, Goodman SB. Revision joint replacement, wear particles, and macrophage polarization. Acta Biomater 2012;8:2815–23. http://dx.doi.org/10.1016/j.actbio.2012.03.042.

[43] Guihard P, Danger Y, Brounais B, David E, Brion R, Delecrin J, et al. Induction of osteogenesis in mesenchymal stem cells by activated monocytes/macrophages depends on oncostatin M signaling. Stem cells 2012;30:762–72. http://dx.doi.org/10.1002/stem.1040.

[44] Nicolaidou V, Wong MM, Redpath AN, Ersek A, Baban DF, Williams LM, et al. Monocytes induce STAT3 activation in human mesenchymal stem cells to promote osteoblast formation. PLoS ONE 2012;7:e39871. http://dx.doi.org/10.1371/journal.pone.0039871.

[45] Yoshida H, Nishikawa M, Yasuda S, Mizuno Y, Toyota H, Kiyota T, et al. TLR9-dependent systemic interferon-β production by intravenous injection of plasmid DNA/cationic liposome complex in mice. J Gene Med 2009;11:708–17. http://dx.doi.org/10.1002/jgm.1348.

[46] Lonez C, Bessodes M, Scherman D, Vandenbranden M, Escriou V, Ruysschaert J-M. Cationic lipid nanocarriers activate Toll-like receptor 2 and NLRP3 inflammasome pathways. Nanomedicine Nanotechnol Biol Med n.d. doi:10.1016/j.nano.2013.12.003.

[47] Zhang G, Guo B, Wu H, Tang T, Zhang B-T, Zheng L, et al. A delivery system targeting bone formation surfaces to facilitate RNAi-based anabolic therapy. Nat Med 2012;18:307–14. http://dx.doi.org/10.1038/nm.2617.